Current Biology 23, 2355–2364, December 2, 2013 ©2013 Elsevier Ltd All rights reserved http://dx.doi.org/10.1016/j.cub.2013.09.060

Article

# The GTPase-Activating Protein RN-tre Controls Focal Adhesion Turnover and Cell Migration

**Andrea Palamidessi,[1,6] Emanuela Frittoli,[1,6] Nadia Ducano,[2,6] Nina Offenhauser,[1] Sara Sigismund,[1] Hiroaki Kajiho,[1] Dario Parazzoli,[1] Amanda Oldani,[1] Marco Gobbi,[3] Guido Serini,[2] Pier Paolo Di Fiore,[1,4,5] Giorgio Scita,[1,5,7,*] and Letizia Lanzetti[2,7,*]**

[1]IFOM, Fondazione Istituto FIRC di Oncologia Molecolare, Via Adamello 16, 20139 Milano, Italy

[2]Dipartimento di Oncologia, Università degli Studi di Torino, Istituto per la Ricerca e la Cura del Cancro, Str. Provinciale 142, 10060 Candiolo, Torino, Italy

[3]Dipartimento di Biochimica e Farmacologia Molecolare, "Mario Negri" Istituto per la Ricerca Farmacologica, 20156 Milano, Italy

[4]Dipartimento di Oncologia Sperimentale, Istituto Europeo di Oncologia, 20141 Milano, Italy

[5]Dipartimento di Scienze della Salute, San Paolo Università degli Studi di Milano, 20122 Milano, Italy

## Summary

**Background:** Integrin-mediated adhesion of cells to the extracellular matrix (ECM) relies on the dynamic formation of focal adhesions (FAs), which are biochemical and mechanosensitive platforms composed of a large variety of cytosolic and transmembrane proteins. During migration, there is a constant turnover of ECM contacts that initially form as nascent adhesions at the leading edge, mature into FAs as actomyosin tension builds up, and are then disassembled at the cell rear, thus allowing for cell detachment. Although the mechanisms of FA assembly have largely been defined, the molecular circuitry that regulates their disassembly still remains elusive.
**Results:** Here, we show that RN-tre, a GTPase-activating protein (GAP) for Rabs including Rab5 and Rab43, is a novel regulator of FA dynamics and cell migration. RN-tre localizes to FAs and to a pool of Rab5-positive vesicles mainly associated with FAs undergoing rapid remodeling. We found that RN-tre inhibits endocytosis of β1, but not β3, integrins and delays the turnover of FAs, ultimately impairing β1-dependent, but not β3-dependent, chemotactic cell migration. All of these effects are mediated by its GAP activity and rely on Rab5.
**Conclusions:** Our findings identify RN-tre as the Rab5-GAP that spatiotemporally controls FA remodeling during chemotactic cell migration.

## Introduction

Engagement of integrin transmembrane receptors with extracellular matrix (ECM) ligands is a central step in the formation of focal adhesions (FAs). These structures are highly dynamic, undergoing a spatiotemporally regulated turnover, particularly during cell migration. In migrating cells, FAs form at the leading edge as nascent adhesions that mature into large FAs through the sequential recruitment of a wide number of components, establishing stable attachment of cells to the substrate. FAs must then disassemble to allow cell rear detachment and effective locomotion [1, 2]. In the past two decades, many molecular details of FA assembly have been identified. Much less is known, however, about the mechanisms and signaling pathways that control FA turnover, a regulatory step that increasing evidence shows to crucially rely on membrane trafficking [3]. FA disassembly, for example, has been found to occur through a targeted mechanism involving microtubules, dynamin, clathrin, and specific clathrin adaptors that locally promote integrin endocytosis [4–8]. Integrin trafficking in the endosomal compartment is controlled by small guanosine triphosphatases (GTPases) of the Rab5 subfamily, Rab5 and Rab21, with the latter playing a crucial role both in integrin endocytosis and recycling [4, 9]. Rab5 is a master regulator of early endosomes [10], where integrins invariably accumulate for subsequent sorting [11]. Recently, Rab5 has also been found to control integrin turnover within long-lived ECM adhesions required for the maintenance of tissue architecture, such as the myotendinous junctions of *Drosophila* embryos [12], and for FA disassembly in some tumor cells [13]. Notably, Rab5 participates in cell migration, not only by regulating integrin internalization [4, 14] but also by promoting endocytic/exocytic cycles of the small GTPase Rac, which is required for spatial resolution of motogenic signals and formation of migratory protrusions [15, 16]. Thus, Rab5 is emerging as a central trafficking molecule that directly influences several aspects of cell migration. How the activity of this small GTPase is regulated during FA turnover and cell migration is, however, still unknown.

Like all small GTPases, the function of Rab5 is controlled by guanine nucleotide exchange factors (GEFs), guanosine nucleotide dissociation inhibitor (GDI), and GTPase-activating proteins (GAPs) [17, 18]. Among the latter proteins, RN-tre, also named USP6NL, has been shown to enhance GTP hydrolysis of Rab5 [19, 20] and more recently also of Rab43, a GTPase involved in transport from the endocytic pathway to the Golgi [21, 22]. Consistent with its biochemical activity on Rab5, RN-tre expression is sufficient to inhibit Rab5-dependent transferrin and epidermal growth factor (EGF) internalization [19]. This endocytic role is evolutionarily conserved from *Drosophila* cells, where RN-tre was identified in a genomic screen for regulators of endocytosis [23], to zebrafish embryos, where RN-tre was shown to inhibit Rab5-dependent endocytosis of Fgf8 [24]. RN-tre also participates in Rab5-dependent signaling to actin dynamics. Ectopic expression of RN-tre, but not its GAP-defective mutant, impairs platelet-derived growth factor (PDGF)-mediated formation of a set of specialized migratory and endocytic actin-based protrusion, commonly referred to as circular dorsal ruffles [20].

Two recent and independent proteomic studies identified RN-tre among the components of FAs [25, 26], but its function in adhesive sites has never been addressed. Here, we set out to investigate this issue further by exploring the role of RN-tre in FA turnover and cell migration.

[6]These authors contributed equally to this work
[7]These authors equally contributed to this work
*Correspondence: giorgio.scita@ifom.eu (G.S.), letizia.lanzetti@ircc.it (L.L.)

## Results

### RN-tre Localizes to Focal Adhesions

RN-tre displays a complex pattern of intracellular localization but is predominantly enriched at the plasma membrane (PM) [20, 27]. We used total internal reflection fluorescence (TIRF) microscopy in living immortalized mouse embryo fibroblasts (MEFs) expressing fluorescently tagged RN-tre to investigate its PM localization in more detail. We observed that RN-tre accumulated in FAs, where it colocalized with two major components of the integrin adhesome, namely vinculin and paxillin (Figure 1A). In addition, RN-tre extensively colocalized in adhesive sites with the ECM-bound/active conformation of β1 integrin, as recognized by the conformation-specific 9EG7 antibody [28] (Figure 1B). Colocalization between RN-tre and active β1 integrin was also evident in fibrillar adhesions, which are structures that are thought to arise from the sliding of active α5β1 heterodimer along actin stress fibers (Figure 1B) [29]. Prompted by this observation, we investigated whether the recruitment of RN-tre to adhesive sites depends on a specific class of integrin. Distinct integrin heterodimers are engaged by different ECM proteins: α5β1 binds to fibronectin and α1β1 and α2β1 to type I collagen, while αvβ3 is mostly engaged by vitronectin [30]. We therefore looked at the localization of RN-tre in fibroblasts plated on these various matrices.

We performed this analysis in fibroblasts derived from *RN-tre* knockout (KO) mice reconstituted with tetracycline-inducible lentiviral vector carrying HA-tagged RN-tre. *RN-tre* KO mice are viable and fertile and do not display gross abnormalities. The knockout strategy and the detailed description for the generation of mice and immortalized fibroblasts are described in Figures S1A–S1F available online. RN-tre was specifically recruited to FAs of cells plated on fibronectin, but not type I collagen or vitronectin (Figures 1C and 1D). Thus, RN-tre localizes to adhesive sites in an α5β1 integrin-dependent manner. Conversely, another known GAP for Rab5, RabGAP-5 [21], displayed a diffuse cytoplasmic distribution, as previously shown [21], and did not accumulate in FAs (Figure S1G).

### RN-tre Regulates β1 Integrin Endocytosis and FA Dynamics

Rab5 activity promotes β1 integrin endocytosis, FA disassembly, and cell adhesion to ECM proteins [4, 13, 14], but how its function is downmodulated during cell adhesion and migration is currently unknown. Thus, we asked whether RN-tre might be a key regulatory molecule of Rab5 in cell adhesion.

First, we evaluated the ability of RN-tre to downregulate Rab5 in vitro, comparing its GAP activity with the one of RabGAP-5. To this end, we measured the catalytic activity of the isolated GAP domains of RN-tre and RabGAP-5 (aa 2–395 for both RN-tre and RabGAP-5) on Rab5 using two independent GAP assays: filter-binding and thin-layer chromatography assays (Figures 2A and 2B; purified proteins used in the assays are shown in Figure S2A). The GAP domains of both these proteins displayed similar and readily detectable GAP activities (Figures 2A and 2B).

To validate the relevance of RN-tre as a GAP for Rab5 in living cells, we measured Rab5-GTP levels in fibroblasts established from *RN-tre* KO and wild-type (WT) embryos. The amount of Rab5-GTP was assessed by taking advantage of the Rab5-binding domain (RBD) of early-endosomal autoantigen 1 (EEA1), a Rab5 effector that binds to active Rab5 on endosomes [31]. The C-terminal RBD of EEA1, which shares homology with the RBD domain of Rabaptin-5 [31], was fused to glutathione S-transferase (GST) and purified, and its ability to interact specifically with the active form of Rab5 was confirmed by using lysates of 293T cells transfected with dominant-active (Rab5Q79L) or dominant-negative (Rab5S34N) Rab5 mutants (Figure 2C). Activation of Rab5 is elicited by EGF stimulation [32]. Similarly, we found that PDGF treatment also stimulates Rab5 activation in a time-dependent fashion (with a peak of activation ~7 min following PDGF stimulation) in *RN-tre* KO primary embryonic fibroblasts (PEFs) (Figure 2D). We then compared the levels of Rab5-GTP in PDGF-stimulated WT or KO PEFs. Since the levels of endogenous active Rab5 were undetectable in WT fibroblasts, we ectopically transfected small amounts of Rab5 into both WT and KO cells. Genetic removal of RN-tre led to a significant increase in the amount of PDGF-induced, GTP-loaded Rab5 (Figure 2E), without altering the levels of expression of the Rab5 effectors, Rabaptin-5 and EEA1 (data not shown). We extended and validated this finding in immortalized *RN-tre* KO MEFs, stably expressing either the inducible empty vector (KO) or WT RN-tre (KO+RN-tre) or the RN-tre GAP-defective mutant RN-tre$^{R150A}$ [19] (KO+RN-treR150A) (Figure 2F). Reexpression of WT RN-tre, but not of RN-tre$^{R150A}$ or the empty vector, impaired PDGF-induced Rab5 activation, indicating that RN-tre is a GAP for Rab5 in vivo (Figure 2G). These results are in line with a previous report showing that overexpression of RN-tre or RabGAP-5 inhibits to a similar extent the levels of Rab5-GTP in PC12 cells [33].

RN-tre is also a GAP for Rab43 [21], the GTP-bound form of which may, therefore, be elevated in *RN-tre* KO MEFs. This, in turn, could stimulate PDGF-dependent loading of GTP on Rab5 via unknown mechanisms. In addition, RN-tre binds, at least in yeast two-hybrid assays, to Rab30 [21]. Hence, we analyzed also Rab30. Expression of dominant-negative Rab43 or Rab30 mutants in *RN-tre* KO MEFs had no effects on Rab5-GTP levels (Figures S2B and S2C). As we currently have no means to measure directly the efficacy of the dominant-negative mutants in reducing the GTP levels of Rab30 and Rab43, our results can only suggest that deregulation of these GTPases unlikely accounts for the increased Rab5 activity of *RN-tre* KO MEFs.

The activation of Rab5 promotes endocytosis and increases the size of early endosomes by stimulating their fusion [34, 35]. Consistently with the higher activity of Rab5 in the *RN-tre* KO cells, the size of Rab5 endosomes appeared to be generally increased in *RN-tre* KO compared to WT fibroblasts (Figure S2D). We previously showed that ectopic expression of RN-tre inhibits the internalization of transferrin and EGF receptors [19]. Thus, we analyzed the kinetics of endocytosis of these receptors in *RN-tre* WT and KO MEFs. As expected for cells in which Rab5 is more active, endocytosis of both receptors was slightly but reproducibly higher in *RN-tre* null cells (Figures S2E and S2F).

Prompted by the localization of RN-tre to FAs, we investigated whether RN-tre might also participate in integrin endocytosis. At the cell surface, integrins are present either in ECM-bound/active or ligand-free/inactive conformations [36]. RN-tre genetic deletion did not significantly alter cell surface levels of either total (i.e., inactive plus active) or active β1 integrin measured by ELISA-based detection after surface biotinylation at 4°C as in [37], under conditions of endocytosis blockade (Figures S3A and S3B). Conversely,

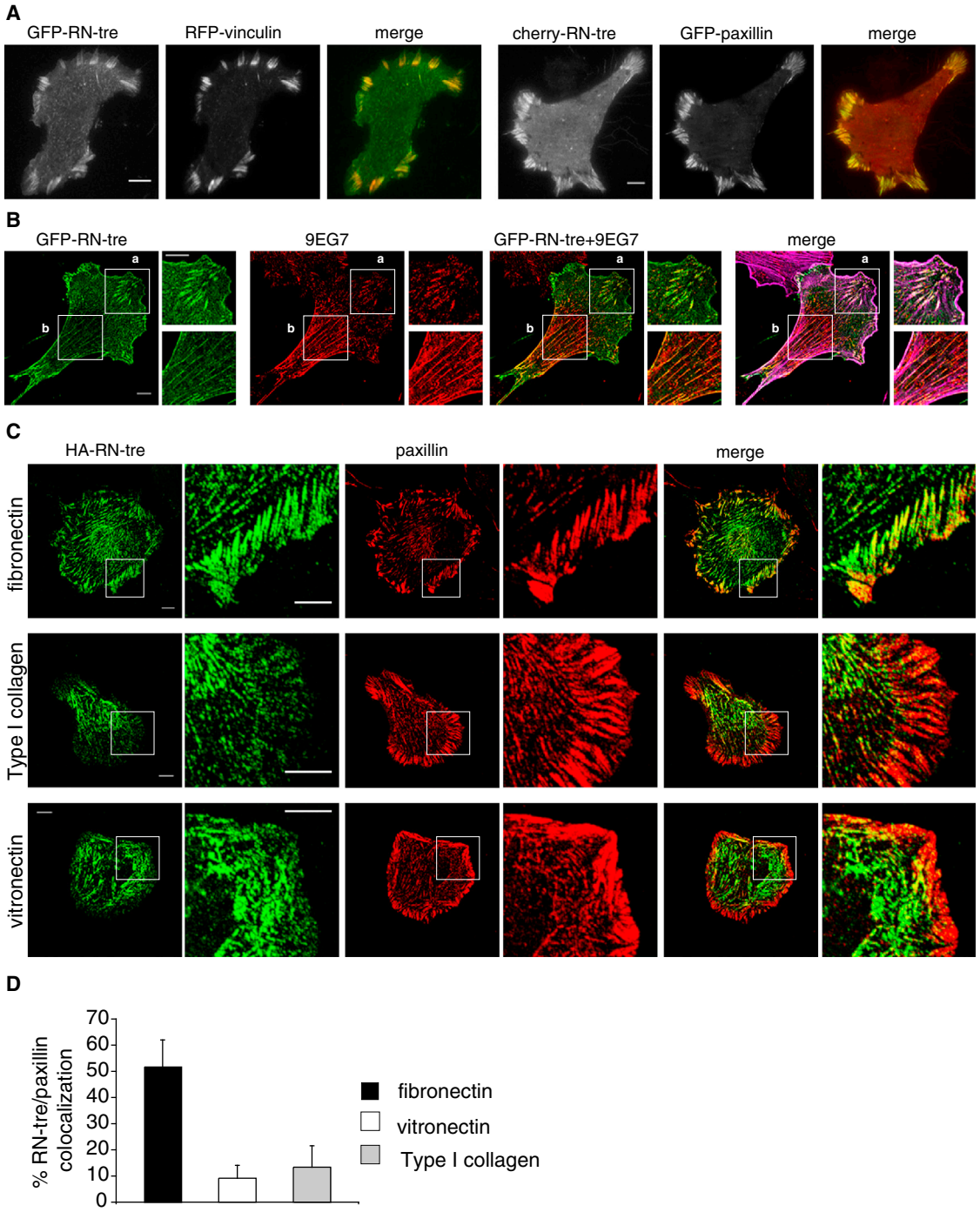


Figure 1. Recruitment of RN-tre to Adhesive Sites

(A) TIRF microscopy of MEFs expressing, in the left panel, GFP-RN-tre (green in merge) and RFP-vinculin (red in merge) and, in the right panel, cherry-RN-tre (red in merge) and GFP-paxillin (green in merge). Scale bars here and in the following figures, unless otherwise specified, represent 10 μm.

(B) Confocal analysis of MEFs expressing GFP-RN-tre (green), stained with a conformation-specific antibody that recognizes the active form of β1 integrin (9EG7, red). Colocalization resulting in yellow staining is evident in the merged image (GFP-RN-tre+9EG7). Actin was revealed by Alexa Fluor 647-conjugated phalloidin (shown in magenta in merge). Regions of the cell corresponding to FAs (a) or fibrillar adhesions (b) are magnified in the insets.

(C) Confocal sections of *RN-tre* KO MEFs transduced with tetracycline-inducible lentiviral vector carrying HA-tagged RN-tre plated on fibronectin (top panel), type I collagen (middle panel), or vitronectin (bottom panel). Cells were allowed to adhere for 4 hr in serum-free medium, fixed, and stained with anti-HA (green) and anti-paxillin (red) antibodies. A region of each cell (boxed) is magnified in the corresponding panels on the right. Colocalization between RN-tre and paxillin is detected only in the cell plated on fibronectin (merge).

(D) Quantification of the experiments in (C) ($n = 5$, mean ± SD; $p < 0.0002$).

See also Figure S1.

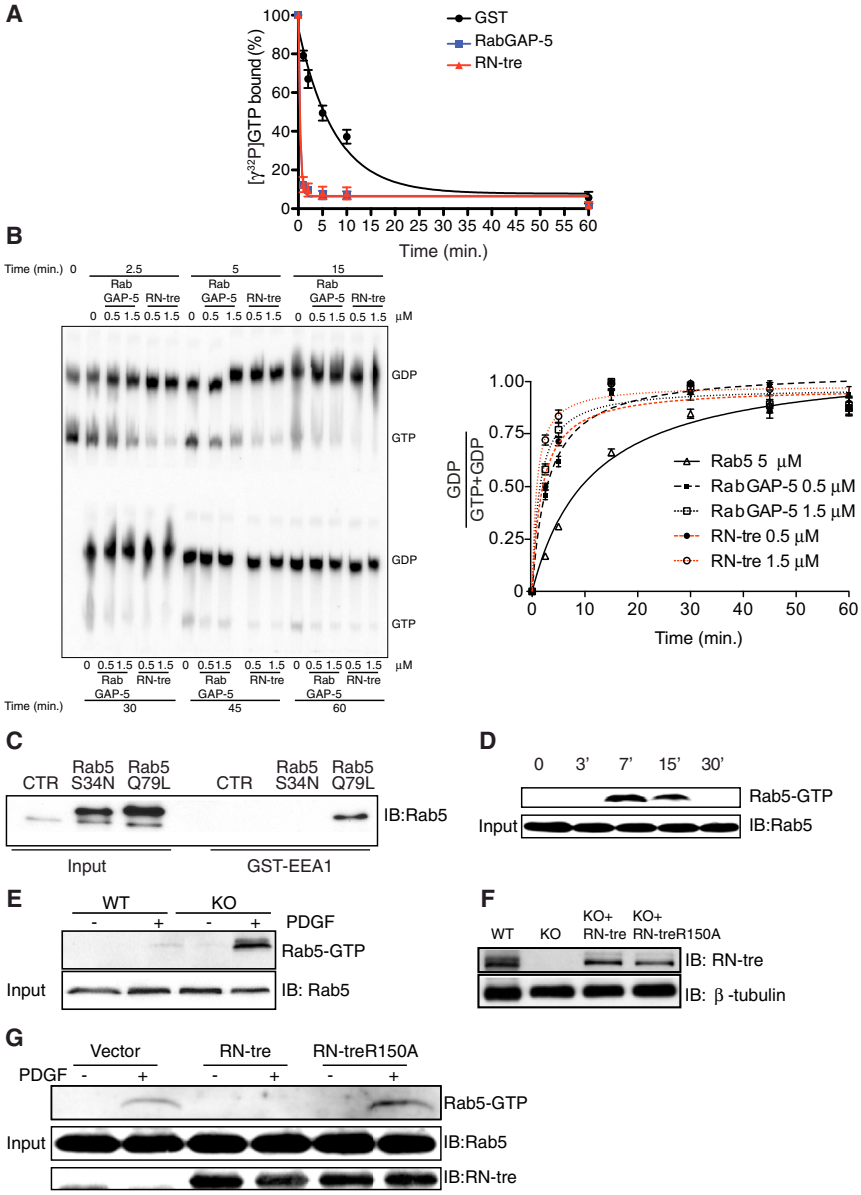


Figure 2. RN-tre GAP Activity toward Rab5

(A) Filter binding GAP assays. [$\gamma$-$^{32}$P]GTP-loaded Rab5 (500 nM) was incubated with 160 nM control GST, GST-RN-tre, or GST-RabGAP-5-GAP domains. GAP activity is expressed as the percentage of nonhydrolyzed [$\gamma$-$^{32}$P]GTP that remained bound to the filters, relative to the radioactivity at time 0. Values are the mean of three independent experiments ± SEM.

(B) Thin-layer chromatography-based GAP assays. [$\alpha$-$^{32}$P]GTP-loaded GST-Rab5 (5 μM) was incubated with the indicated concentrations of the GST-GAP domains of either RabGAP-5 or RN-tre. At various time points, Rab5-associated nucleotides were separated by PEI-cellulose thin-layer chromatography (Merck Biosciences). Left panel: representative autoradiography from five independent experiments with similar results. Note that the amount of [$\alpha$-$^{32}$P]GDP at time 0 derives from intrinsic hydrolysis of Rab5 despite that we used ice-cold temperatures for the loading reaction (see also Supplemental Experimental Procedures for additional details). Right panel: quantification of the experiments with Typhoon Trio. The density of the signal corresponding to the [$\alpha$-$^{32}$P]GDP produced at various time points of the hydrolytic reaction was quantified with ImageJ after subtracting the signal density of [$\alpha$-$^{32}$P]GDP present in the preparation of [$\alpha$-$^{32}$P]GTP-loaded GST-Rab5 before the start of the reaction (first lane). Data are expressed as the fraction of [$\alpha$-$^{32}$P]GDP produced during hydrolysis over total nucleotide ([$\alpha$-$^{32}$P]GTP + [$\alpha$-$^{32}$P]GDP) and are the mean ± SEM of three independent experiments run in triplicates.

(C) Total cellular lysates from 293T cells transfected with the indicated constructs (CTR, mock transfection) were incubated with GST-EEA1 (GST-EEA1 lanes). Immunoblotting (IB) was performed with anti-Rab5 antibody. Input lysates (50 μg) are also shown.

(D) Input lysates of *RN-tre* KO PEF transfected with CFP-Rab5 and stimulated with PDGF for the indicated times were subjected to GST-EEA1 assay and IB as indicated.

(E) Input lysates of WT or KO PEF transfected with CFP-Rab5 and stimulated with PDGF for 7 min, as shown on top, were subjected to GST-EEA1 assay and IB as indicated.

(F) Total lysates of WT or KO MEFs transduced with tetracycline-inducible lentiviral vectors carrying either RN-tre (KO+RN-tre) or its GAP-defective mutant RN-treR$^{150A}$ (KO+RN-treR150A) or empty vector (KO). Cells were treated with doxycycline (0.5 μg/ml) for 48 hr to express the proteins. Lysates were IB as indicated.

(G) *RN-tre* KO MEFs expressing empty vector (KO), RN-tre (KO+RN-tre), or RN-tre$^{R150A}$ (KO+RN-treR150A) were transfected with CFP-Rab5 before PDGF (+) or mock (−) stimulation for 7 min. Input lysates were subjected to GST-EEA1 assay and IB as indicated. Notably, the same amounts of ectopically expressed CFP-Rab5, as witnessed by its levels detected in input lysates by immunoblotting, were used in all these assays.

See also Figure S2.

the internalization rates of both total and active β1 integrin were increased in the *RN-tre* KO MEFs compared to WT cells (Figure 3A). We also tested the effects of RN-tre removal on the endocytosis of β3 integrin, but in this case, no differences were detected between WT and KO fibroblasts (Figure 3B). This result is consistent with findings that RN-tre is specifically recruited to FAs of cells plated on fibronectin, but not vitronectin, which respectively bind with high affinity to α5β1 and αvβ3 integrins (Figures 1C and 1D). Reexpression of RN-tre in KO MEFs robustly reduced the rate of β1 integrin endocytosis, whereas the GAP-defective mutant did not (Figure S3C), thus indicating that the GAP activity of RN-tre controls the endocytosis of β1 integrin, as previously shown for other PM receptors ([19]; Figures S2E and S2F).

Integrin endocytosis is a mechanism that allows for FA disassembly [5, 7, 8]. Accordingly, Rab5 participates in β1 integrin trafficking [4, 14] and adhesion turnover in mammalian tumor cells [13] and in *Drosophila* myotendinous junctions [12]. Having found that RN-tre is in FAs and regulates β1 integrin endocytosis, we tested its ability to control FA turnover. To this end, WT and KO MEFs were transfected with GFP-paxillin to monitor adhesion dynamics by fluorescence recovery after photobleaching (FRAP) analysis. We analyzed FAs located at the cell periphery or at the cell rear, and also

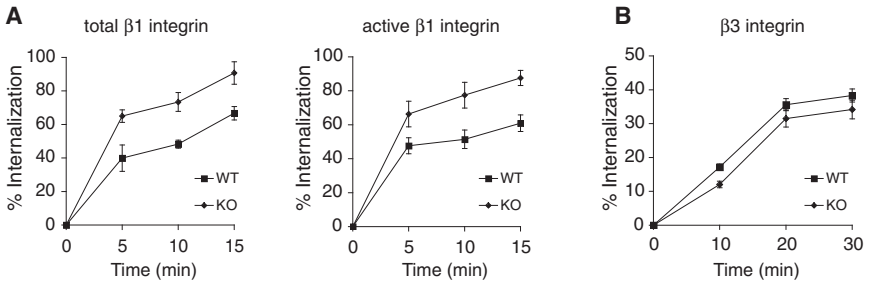


Figure 3. RN-tre Participates in β1 Integrin Endocytosis

*RN-tre* KO and WT MEFs were surface labeled with cleavable biotin. Integrin internalization was allowed for the indicated times, and biotin present on the cell surface was cleaved. The amount of biotinylated intracellular total (A, left) or active β1 integrin (A, right) or β3 integrin (B) was determined by ELISA. Data are expressed as the percentage of internalized receptor, relative to the total amount of cell surface-labeled receptor (n = 3, mean ± SD; $p < 0.002$ in A). See also Figure S3.

fibrillar adhesions (Figures 4A–4C). Typically, two to four GFP-paxillin-positive FAs were analyzed per cell. The mean half-time of fluorescence recovery (FRAP t1/2) in the bleached area was determined as an estimate of the stability of adhesion binding. KO MEFs exhibited a significantly faster recovery of GFP-paxillin compared to WT both in peripheral FAs (mean FRAP t1/2 KO, 18.3 ± 1.6 s versus FRAP t1/2 of WT, 32.6 ± 2.2 s) (Figure 4A; Movie S1) and in FAs at the cell rear (mean FRAP t1/2 of KO, 15.6 ± 1.2 s versus FRAP t1/2 of WT, 27.5 ± 2.3 s) (Figure 4B; Movie S1). No significant differences were scored in the turnover of fibrillar adhesions (Figure 4C; Movie S1). Reexpression of RN-tre, but not of RN-tre$^{R150A}$, severely affected GFP-paxillin turnover in peripheral FAs (mean FRAP t1/2 of KO, 18.7 ± 2.8 s versus FRAP t1/2 of KO+RN-tre, 44.5 ± 3.7 s and FRAP t1/2 KO+RN-treR150A, 17.5 ± 3 s) (Figure 4D; Movie S2). These results strengthen our findings that removal of RN-tre increases β1 integrin endocytosis in a GAP-dependent manner, further predicting that faster fluorescence recovery of GFP-paxillin in the KO MEFs might depend on higher levels of active Rab5. To verify this prediction, we silenced all the three isoforms of Rab5 (Rab5A/Rab5B/Rab5C), which act redundantly in endocytosis [38], or Rab43 in KO MEFs transfected with GFP-paxillin (Figures S4A and S4B). Peripheral GFP-paxillin-positive FAs were subjected to FRAP analysis. Silencing of Rab43 left unperturbed the FRAP t1/2 of KO MEFs (19.3 ± 1 s in Rab43 knockdown [KD] versus 15.4 ± 1.2 s in KO MEFs silenced with control oligos) (Figure 4E; Movie S2). Instead, interference with Rab5 isoforms significantly delayed GFP-paxillin turnover (FRAP t1/2, 34.2 ± 2.1 s) (Figure 4E; Movie S2). Collectively, these results indicate that RN-tre inhibits FA turnover likely via its GAP activity toward Rab5, but not toward Rab43.

To investigate further the role of RN-tre in FA dynamics, we performed a structure-function analysis identifying the region of RN-tre responsible for targeting to FAs and looking at the ability of the RN-tre mutant, which does not accumulate in FAs, to alter GFP-paxillin turnover. Progressive deletion of the RN-tre C terminus revealed that the mutant encompassing the first 395 amino acids of RN-tre (RN-tre-1–395), which retains the GAP domain, localized to the PM but did not accumulate in FAs (Figures 5A and 5B). Microinjection of this mutant in KO MEFs had no effect on GFP-paxillin turnover, under conditions in which full-length RN-tre significantly delayed the recovery of GFP-paxillin (Figures 5C, 5D, and S4D). These results suggest that the GAP activity of RN-tre needs to concentrate in FAs to efficiently inhibit their turnover.

To provide additional support to the hypothesis that RN-tre controls the dynamics of FA remodeling by interacting with Rab5, we monitored the localization of RN-tre and Rab5 in FAs by live TIRF microscopy. We expressed GFP-RN-tre, RFP-Rab5, and CFP-paxillin in *RN-tre* KO MEFs and looked at their localization during cell spreading on fibronectin, when adhesions are highly dynamic. Rab5 was primarily present, as expected, in vesicles, whereas RN-tre was both in FAs and on vesicles (Figure 5E; Movie S3). Strikingly, we detected colocalization of RN-tre and Rab5 on vesicles that were mainly associated with FAs undergoing rapid remodeling (Movie S3).

### Genetic Deletion of RN-tre Enhances Cell Migration

Flux of integrins through the endocytic pathway and FA turnover dictate the speed of cell migration ([39]; reviewed in [11]); we thus investigated the effects of RN-tre removal on cell migration on ECM substrates. We initially tested random cell motility in primary fibroblasts from WT and KO littermate embryos, using Dunn chamber assays, in the absence of any diffusible gradient. Under these conditions, both the total distance and cell velocity were increased in fibroblasts lacking RN-tre as compared to WT cells, while directionality, which measures the ability of a cell to move persistently along its migratory path, was not significantly altered (Figure 6A). These results suggest that RN-tre removal fosters the speed of cell migration, consistent with its role in regulating FA turnover. Next, we used the same Dunn chamber setting but added PDGF to one of the wells to generate a diffusible gradient and investigated chemotactic migration of RN-tre- or RN-tre$^{R150A}$-expressing or control KO MEFs. PDGF is a potent motogenic factor for fibroblasts that also induces Rab5 activation in a RN-tre-dependent manner (Figures 2E and 2G). As expected, genetic deletion of RN-tre increased both the distance and the velocity without affecting the persistency of random cell migration (Figure 6B; Movie S4). Instead, reexpression of RN-tre, but not of the GAP-defective mutant, had a dramatic inhibitory effect on the ability of cells to move toward the PDGF gradient, as witnessed by the ~10-fold reduction in forward migration index (Figure 6B; Movie S4).

RN-tre removal increases the levels of active Rab5 in response to PDGF stimulation (Figure 2E). We therefore investigated whether this small GTPase, rather than other RN-tre targets, is responsible for the altered chemotactic cell migration by silencing all Rab5 isoforms simultaneously, or Rab43 or Rab30 (Figures 6C and S4A–S4C; Movie S4). Silencing of Rab5 isoforms severely impaired distance, velocity, and forward migration index of *RN-tre* KO MEFs (Figure 6C; Movie S4) as well as of reconstituted cells (data not shown). Conversely, silencing of Rab43 or Rab30 had no appreciable effects on any of the migratory parameters measured (Figure 6C; Movie S4).

RN-tre removal also significantly improved the forward migration of cells plated on fibronectin, but not on vitronectin (Figures S5A and S5B; Movie S5). This result is consistent with (1) the specific recruitment of RN-tre to FAs of cells plated

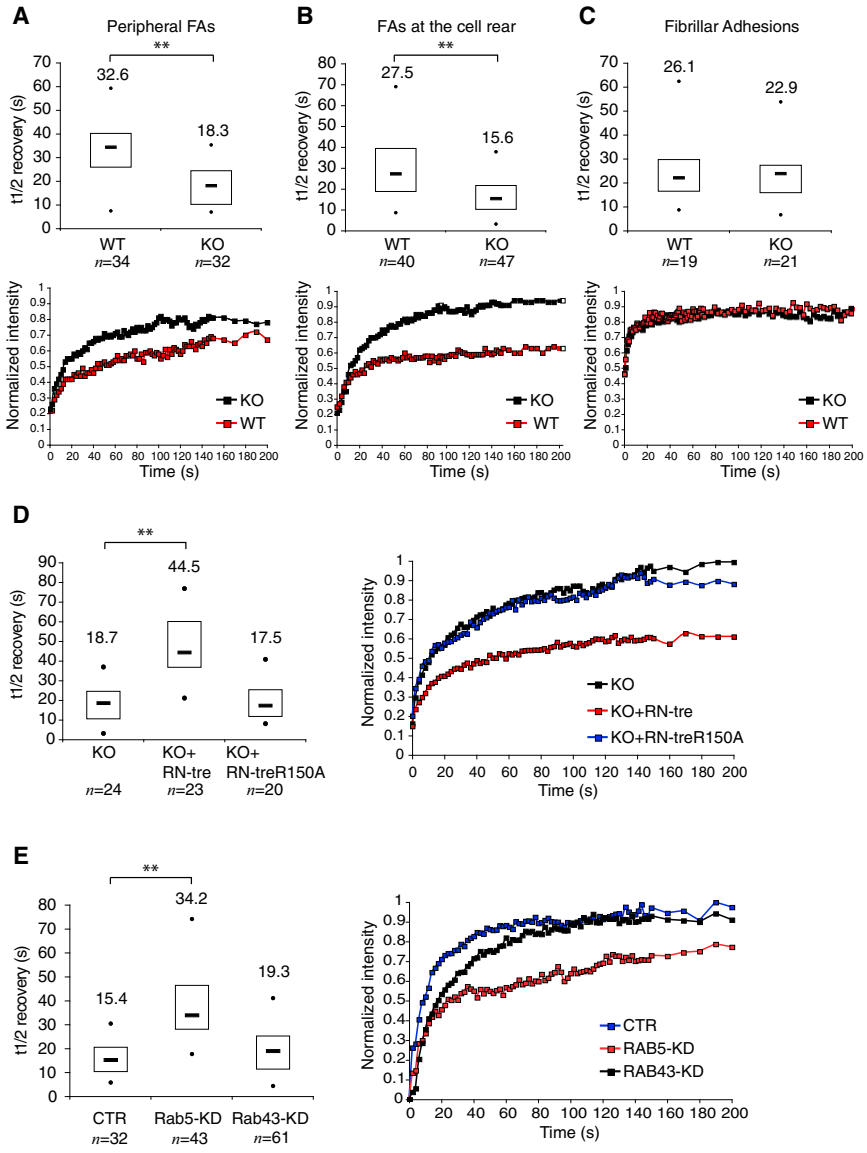


Figure 4. RN-tre Controls FA Turnover

*RN-tre* WT and KO MEFs (A–C), KO MEFs expressing or not expressing RN-tre or RN-treR$^{150A}$ (D), or KO MEFs silenced with Rab5A, Rab5B, Rab5C, or Rab43 or control oligos (CTR) (E) were transfected with GFP-paxillin. GFP-paxillin-positive adhesions, in the various cell populations, were subjected to FRAP analysis, and results showing the half-time of fluorescence recovery are reported in the box plots. n is the number of FAs analyzed in each sample. The mean FRAP t1/2 in seconds is indicated above each box; **p < 0.001. Sample fluorescence recovery curves of FRAP are shown below each plot in (A)–(C) or reported on the right in (D) and (E). The fluorescence intensity in the recovery curves corresponds to the fluorescence at each time point after photobleaching, background subtracted, and normalized to the prebleaching intensity of 1.

(A–C) FRAP of peripheral FAs (A), FRAP of adhesions at the cell rear (B), and FRAP of fibrillar adhesions (C).

(D) FRAP analysis of GFP-paxillin-peripheral FAs in *RN-tre* KO MEFs expressing empty vector (KO), RN-tre (KO+RN-tre), or RN-treR$^{150A}$ (KO+RN-treR150A).

(E) FRAP analysis of GFP-paxillin-peripheral FAs in *RN-tre* KO MEFs silenced with control oligos (CTR), oligos for Rab5 (Rab5 KD), or oligos for Rab43 (Rab43 KD). RNAi cells were analyzed for mRNA content by qRT-PCR (Figures S4A and S4B).

See also Figure S4 and Movies S1 and S2.

on fibronectin, but not vitronectin, and (2) the effects of RN-tre on the endocytosis of the main fibronectin receptor, $\alpha5\beta1$ integrin, but not on the vitronectin receptor, $\alpha v\beta3$ integrin. Finally, ectopic expression of RN-tre in HeLa cells impaired EGF-directed cell migration, suggesting that RN-tre is generally implicated in growth factor-mediated motility (Figure S5C; Movie S6). Of note, silencing of RabGAP-5 in NIH 3T3 fibroblasts did not alter migratory parameters of fibroblasts moving toward a chemotactic gradient of PDGF (Figures S5D and S5E; Movie S7).

Collectively, our findings indicate that RN-tre, by specifically targeting Rab5-mediated $\beta1$ integrin endocytosis and FA dynamics, is a critical regulator of chemotactic cell migration.

## Discussion

Spatiotemporal control of FA turnover is essential to support cell migration [1, 2]. Our study uncovers RN-tre as a novel and physiologically relevant component of FAs that participates in their turnover by controlling Rab5-dependent dynamic association of key FA adaptors, like paxillin, and the endocytosis of essential FA components, such as $\beta1$ integrin, ultimately impacting on cell migration.

We found that, in accordance with the ability of RN-tre to stimulate GTP hydrolysis on Rab5 ([19] and this study), genetic removal of RN-tre increases the levels of active Rab5 in fibroblasts fostering cellular processes that depend on Rab5 activation, such as $\beta1$ integrin endocytosis. In agreement with endocytosis of integrins as a mechanism to control FA disassembly and cell motility [11, 41], *RN-tre* KO fibroblasts display faster FA turnover and increased cell migration. It is of note that the forward migration index, a parameter that expresses the ability of cells to migrate along with a chemotactic gradient, is improved in *RN-tre* KO fibroblasts, indicating that RN-tre is a relevant player in chemotactic migration of mammalian cells. This is also supported by recent findings showing that RN-tre participates in the directional migration of border cells in *Drosophila melanogaster* [42], a migratory process in which Rab5 is pivotal [43].

RN-tre is also a GAP for Rab43 [21, 22]. However, the regulation of Rab43 by RN-tre does not seem to be essential for cell migration, because silencing of Rab43 does not affect FA turnover or the migratory capabilities of the *RN-tre* KO fibroblasts. Conversely, silencing of Rab5 abrogates all these effects, indicating that they rely on Rab5. Despite these findings, we cannot exclude that RN-tre might also act in cell migration by regulating other Rabs in addition to Rab5.

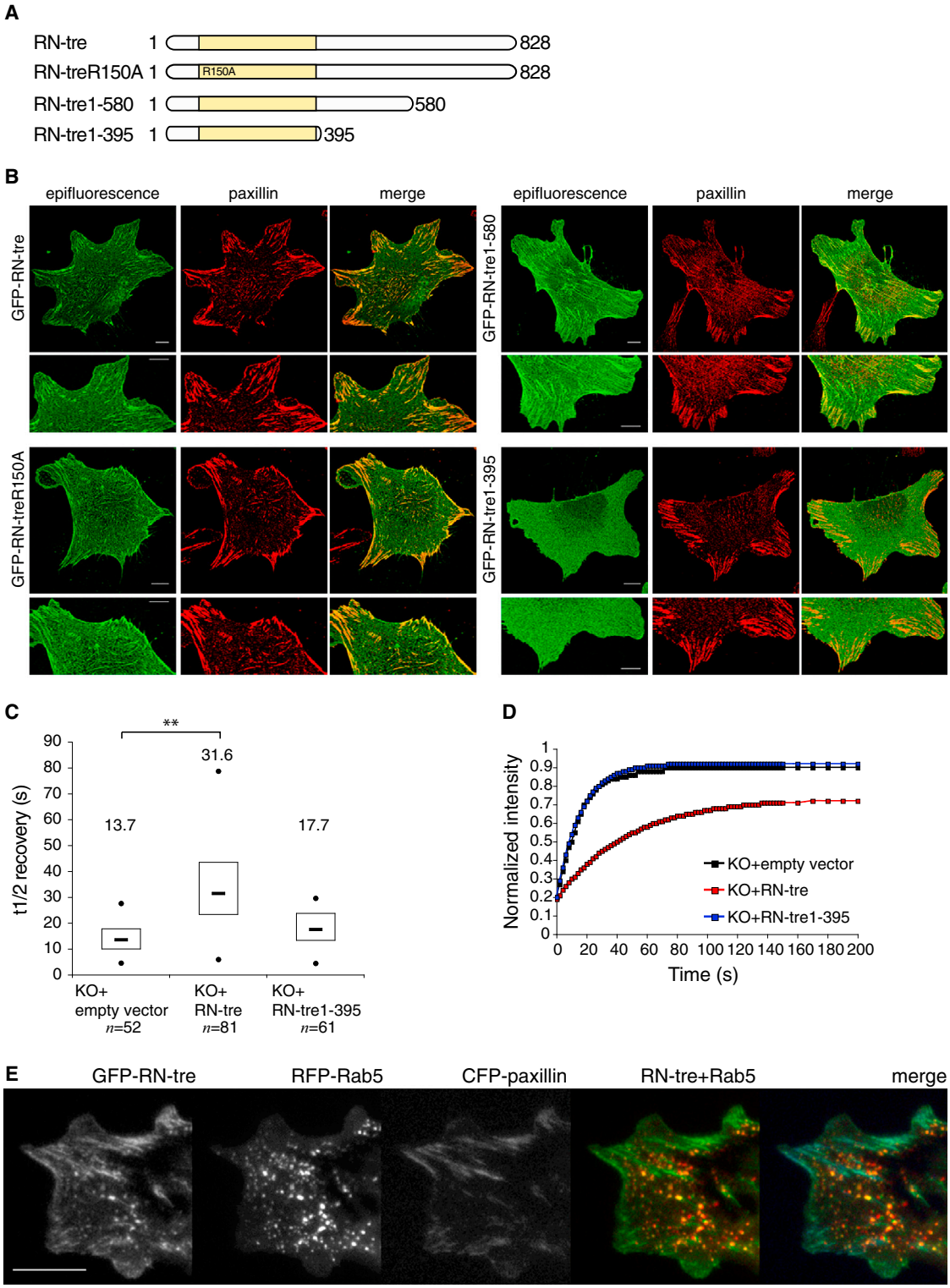


Figure 5. Localization of RN-tre to FAs Is Required to Regulate Their Turnover

(A) Scheme of RN-tre and its mutants. The GAP domain is indicated by a yellow box.

(B) *RN-tre* KO MEFs were transfected with the GFP-tagged constructs indicated on the left of each panel and stained with paxillin. Confocal images show the GFP epifluorescence in green and paxillin staining in red. Lower panels are magnifications of the corresponding upper panels. Colocalization between paxillin and RN-tre or RN-treR$^{150A}$ or RN-tre1–580 results in yellow staining in the merge. No specific accumulation in paxillin-positive FAs could be detected for RN-tre1–395.

(C) *RN-tre* KO MEFs were comicroinjected with GFP-paxillin and empty vector (KO+empty vector), HA-tagged RN-tre (KO+RN-tre), or HA-RN-tre1–395 (KO+RN-tre1–395) and subjected to FRAP analysis. Coexpression of GFP-paxillin and HA-RN-tre or HA-RN-tre1–395 is shown in Figure S4D. The box plot shows the t1/2 of GFP-paxillin fluorescence recovery. n is the number of FAs analyzed in each sample. The mean FRAP t1/2 in seconds is indicated above each box; **p < 0.001.

*(legend continued on next page)*

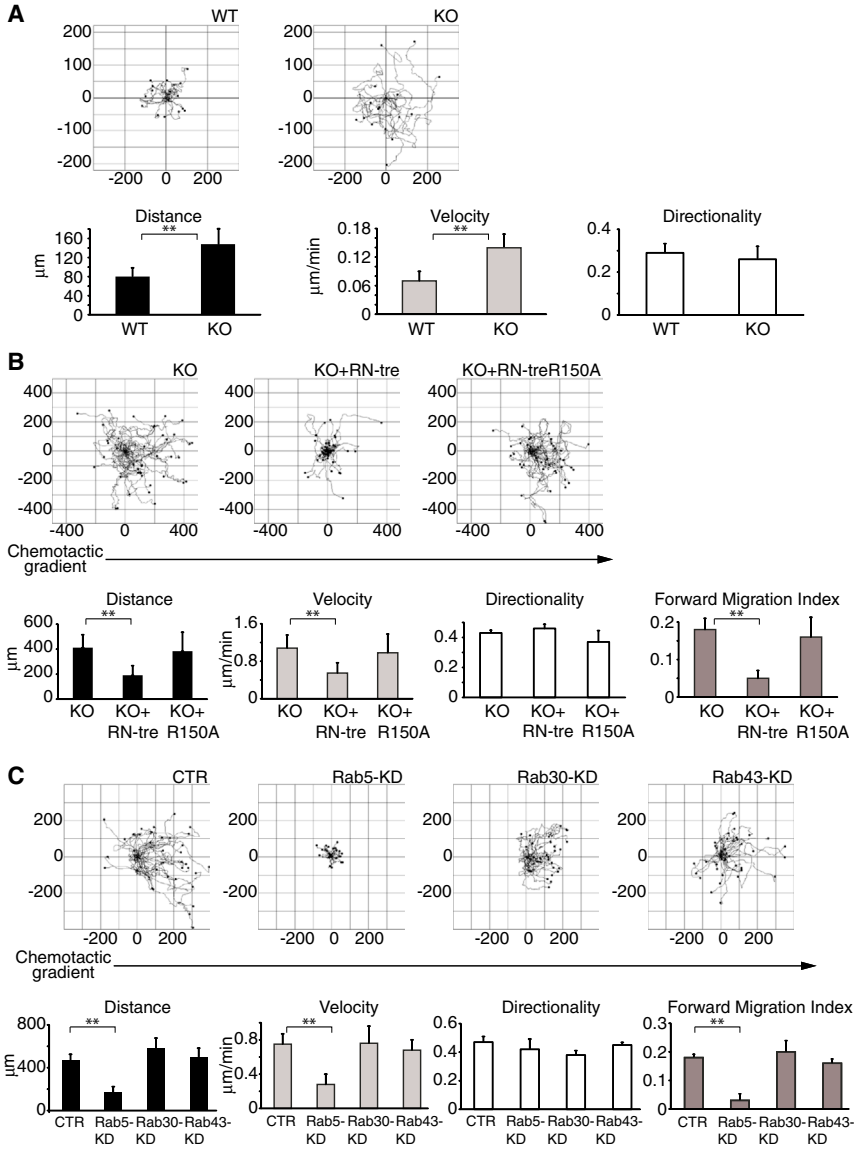


Figure 6. RN-tre Regulates Cell Motility and Chemotactic Migration through Its GAP Activity toward Rab5

(A) PEFs derived from *RN-tre* WT or KO littermate embryos were analyzed in Dunn chamber assays in the absence of any diffusible gradient. Random cell migration was tracked every 5 min interval over a 16 hr period. The migratory tracks of some representative cells are shown for WT and KO PEFs. Tracking of cells was performed by using the "manual tracking" and "chemotaxis and migration tool" ImageJ plugins. Various migration parameters obtained by monitoring at least 30 single cells/experiment/genotype are plotted in the graphs below; $^{**}p < 0.01$.

(B) *RN-tre* KO MEFs expressing or not expressing RN-tre or RN-tre$^{R150A}$ were analyzed for chemotactic migration over a diffusible PDGF gradient in Dunn chamber assays. The migratory tracks of some representative KO, KO+RN-tre, and KO+RN-treR150A MEFs were determined as described above. Migration parameters of at least 60 single cells/experiment/condition are plotted in the graphs below. The forward migration index represents the efficiency of forward migration of cells on the axis parallel to the direction (indicated by the arrow) of a chemotactic gradient. It is calculated by dividing the net distance covered by a cell in the direction of the chemotactic migration axis (Xc) per the total accumulated distance (Dc), as described in [40].

(C) KO MEFs were transfected with a mix of RNAi against Rab5A, Rab5B, and Rab5C, with a single RNAi against Rab43 or Rab30, or with scrambled RNAi (used as control, CTR) and subjected to Dunn chamber assays, as described in (B). The migratory tracks of representative control and Rab-interfered MEFs are shown. Various migration parameters obtained by monitoring at least 50 single cells/experiment/condition are plotted in the graphs below; $^{**}p < 0.01$.

See also Figure S5 and Movies S4, S5, S6, and S7.

Rab5, like other small GTPases, displays multiple GEFs and GAPs [17, 18]. Among them, RN-tre, but not the other major GAP for Rab5, RabGAP-5, is recruited to FAs and inhibits cell migration, whereas the Rab5 GEF RIN2, which also localizes to adhesive sites, promotes cell adhesion and motility [14]. This suggests that at adhesive sites, a molecular circuitry, made by positive and negative regulators of Rab5, controls the function of this small GTPase during cell migration. This hypothesis is also supported by evidence that RN-tre localizes to a pool of Rab5-positive vesicles that are in close proximity to the PM, preferentially associated with remodeling FAs.

Of note, RN-tre controls β1, but not β3, integrin endocytosis and accordingly regulates the directional migration of cells plated on fibronectin, the major α5β1 integrin ligand, but not on vitronectin, which mainly engages αvβ3 integrin. This specificity likely relies on the preferential recruitment of RN-tre to FAs of cells plated on fibronectin, but not on vitronectin, implicating α5β1 in the localization of RN-tre to adhesive sites. These data further strengthen the notion that recruitment of RN-tre to FAs is a distinguished feature of this GAP that specifies its function in directional cell migration. In conclusion, RN-tre acts as a "brake" in cell motility: by turning off Rab5, it inhibits β1 integrin endocytosis and favors FA stability, shifting the balance between adhesion and migration toward a less motile phenotype.

### Experimental Procedures

All animal experiments were performed in accordance with national and international laws and policies. Mice were bred and housed under pathogen-free conditions in our animal facilities at Cogentech Consortium at the FIRC Institute of Molecular Oncology Foundation and at the European Institute of Oncology in Milan.

(D) Sample fluorescence recovery curves of FRAP.

(E) Snapshot from live TIRF imaging of a region of a *RN-tre* KO cell expressing GFP-RN-tre (green in merge), RFP-Rab5A (red in merge), and CFP-paxillin (blue in merge). Cells were plated on fibronectin (2 μg/ml) for 40 min before imaging. Merge of GFP-RN-tre and RFP-Rab5 is also shown (RN-tre+Rab5). Rab5 and RN-tre colocalize on a pool of vesicles closely associated to FAs.

See also Movie S3.

### Generation of *RN-tre* Null Mice

We generated *RN-tre* knockout mice by targeting exon 7 and exon 8 of the *RN-tre* gene that encode for a portion of the GAP domain, including Arg150, which is essential for the catalytic activity of RN-tre [19]. A schematic representation of the strategy is presented in Figures S1A–S1F. Immortalized fibroblasts from *RN-tre* WT or KO embryos were established as described previously [44].

### Cell Culture

Primary and immortalized embryo fibroblasts were grown in DMEM (Lonza) supplemented with 10% South American Serum (EuroClone) and 1% L-glutamine (EuroClone); when indicated, cells were plated on the following matrices: fibronectin (F0895), vitronectin (V8379), and type I collagen (C4243) (5 μg/ml; Sigma-Aldrich). Transfections were performed using Lipofectamine Plus (Invitrogen) according to the manufacturer's instructions. Serum-starved MEFs were stimulated with 10 ng/ml of PDGF (R&D Systems). KO MEFs were reconstituted with RN-tre or RN-tre$^{R150A}$ using tetracycline-inducible lentiviral vectors and grown in DMEM supplemented with 10% Tet system-approved FBS (Clontech). Expression of RN-tre or RN-tre$^{R150A}$ was achieved by adding doxycycline (0.5 μg/ml; Sigma-Aldrich) 48 hr before harvesting cells.

### Imaging Techniques and Quantifications

Immunofluorescence was performed as in [45]. Primary antibodies were revealed by Alexa Fluor 555 and 488 (Molecular Probes)-conjugated secondary antibodies. Confocal analysis was performed on a Leica TCS SP2 AOBS microscope and processed in Adobe Photoshop. Quantitative analyses of colocalization between RN-tre and paxillin were performed with ImageJ software (http://rsb.info.nih.gov/ij/). Images were taken with identical settings, and a mask with fixed threshold that identifies paxillin-positive FAs was applied to all images. The mean pixel intensity in these areas was measured in the green channel (RN-tre) and in the red channel (paxillin), and the intensity of paxillin was used for normalization.

TIRF microscopy was performed using a Leica AM TIRF MC system mounted on a Leica AF 6000LX workstation on living cells. Cells were plated onto glass-bottom dishes (WillCo-dish; Willcowells) and placed onto a sample stage within an incubator chamber set to 37°C, in an atmosphere of 5% $CO_2$, 20% humidity. A 63×/1.40 NA oil-immersion objective was used, and laser penetration depth was set at 110 nm. Excitation and analysis of fluorescent proteins were performed with a 488 nm (for GFP), 532 nm (for cherry or RFP), or 405 nm laser (for CFP-paxillin). Imaging was recorded on a Hamamatsu EM-CCD camera (C9100-02). For experiments of colocalization of GFP-RN-tre, RFP-Rab5A, and CFP-paxillin, controls were performed transfecting cells with single constructs that were filmed under the same conditions used for the cells simultaneously transfected with the three constructs in order to verify the absence of crosstalk among the channels. FRAP was performed on an UltraVIEW VoX spinning-disk confocal system (PerkinElmer) equipped with an EclipseTi inverted microscope (Nikon) provided with a Nikon Perfect Focus System, an integrated FRAP PhotoKinesis unit (PerkinElmer), and a Hamamatsu EM-CCD camera (C9100-50) and driven by Volocity software (Improvision; Perkin Elmer).

Cells were placed in an environmental microscope incubator (OKOLab) set to 37°C and 5% $CO_2$ perfusion. All images were acquired through a 60× oil-immersion objective (Nikon Plan Apo VC, NA 1.4). WT and KO MEF populations and KO MEFs either treated with doxycycline or silenced with siRNA oligos (as described in legend to Figure 4) were transiently transfected with GFP-paxillin 24 hr before FRAP. Several bleach regions with a size of 4 × 2.2 μm were positioned on selected peripheral FAs or on adhesions at the cell rear. Photobleaching was performed using 50 iterations with the 50 mW solid-state 488 nm laser set to maximum power. To determine the recovery kinetics of peripheral adhesions, postbleaching images were recorded for 200 s: the first 150 s with a speed of 0.5 frame/s and then of 0.1 frame/s. For adhesions at the cell rear, postbleaching images were recorded with a speed of 0.5 frame/s for the first 154 s and then 0.2 frame/s. In the case of fibrillar adhesions, which are thin elongated structures, in order to minimize the photobleaching of GFP-paxillin in the cytoplasm, the size of bleach regions was set to 5 × 1.5 μm, and the postbleaching recovery was recorded for 200 s, the first 70 s with a speed of 1 frame/s and then 0.3 frame/s. Quantitative analyses were performed with ImageJ software: the mean intensity values over time were measured, background subtracted, and corrected for acquisition photobleaching. A single exponential function was used to fit the recovery curves of peripheral FAs and adhesions at the cell rear. For fibrillar adhesions, a double exponential fitting was used. In the experiments shown in Figures 5C and 5D, plasmids carrying GFP-paxillin and HA-RN-tre, HA-RN-tre1–395, or pCDNAHA (molar ratio between the two plasmids was 1:2) were comicroinjected 16 hr before performing FRAP analysis.

### Dunn Chamber Assays

Cells were seeded onto a suitably washed sterile coverslip and allowed to settle prior to assembling the chemotaxis chamber. Initially, both annular wells were filled with medium supplemented with 0.5% South American Serum, and the coverslip seeded with cells was inverted onto the chamber in an offset position in order to leave a narrow filling space at one edge for access to the outer well. The coverslip was sealed in place using hot orthodontic wax applied with a paintbrush around all the edges except for the filling space. The medium in the outer well was replaced with medium containing 10 ng/ml PDGF or 100 ng/ml EGF for migration of HeLa cells. The chamber was incubated at 37°C, 5% $CO_2$, and images were taken with a Nikon Eclipse TE2000-E inverted microscope.

### Integrin Internalization Assays

Integrin endocytosis assays were performed as described previously [37]. Briefly, cells were transferred to ice, washed twice in cold PBS, and surface labeled at 4°C with 0.5 mg/ml sulfo-NHS-SS-biotin (Thermo Scientific) in PBS for 30 min. Labeled cells were washed twice with ice-cold DMEM 1% FBS and twice with ice-cold PBS and transferred to prewarmed DMEM 1% FBS at 37°C containing 0.2 mM primaquine, an antimalaria drug known to inhibit recycling of membrane and membrane-bound molecules to the PM from endosomes. At the indicated times, dishes were rapidly transferred to ice and washed twice with ice-cold PBS. Biotin was removed from proteins remaining at the cell surface by incubation with a solution containing 20 mM sodium 2-mercaptoethanesulfonate (MesNa) in 50 mM Tris-HCl (pH 8.6), 100 mM NaCl, 0.015 N NaOH for 1 hr at 4°C. MesNa was quenched by the addition of 20 mM iodoacetamide for 10 min, and after two further washes in PBS, the cells were lysed in 25 mM Tris-HCl (pH 7.6), 100 mM NaCl, 2 mM $MgCl_2$, 1 mM $Na_3VO_4$, 0.5 mM EGTA, 1% Triton X-100, 5% glycerol, protease inhibitor cocktail (Sigma-Aldrich), and 1 mM PMSF. Lysates were cleared by centrifugation at 12,000 × *g* for 20 min. After correction to equivalent protein concentrations, the levels of biotinylated β1 integrin were determined by capture-ELISA as in [37]. Antibodies used in the ELISAs were mouse anti-β1 integrin (Abcam; ab30388), rat anti-active β1 integrin 9EG7 (BD Pharmingen; 550531), or mouse anti-β3 integrin (BD Pharmingen; 555752).

Further detailed experimental procedures, including expression vectors and antibodies, RNAi silencing, protein purification, GAP assays, pull-down assays for detection of Rab5-GTP, transferrin and EGF saturation binding, and internalization assays are provided in the Supplemental Experimental Procedures.

### Supplemental Information

Supplemental Information includes five figures, Supplemental Experimental Procedures, and seven movies and can be found with this article online at http://dx.doi.org/10.1016/j.cub.2013.09.060.

### Acknowledgments

We thank David Lambright for assistance with GAP assays. Work in the authors' lab is supported by grants from the Associazione Italiana per la Ricerca sul Cancro (P.P.D.F. and G. Scita; START UP program #6310 to L.L.), the European Community (FP7) (P.P.D.F.), the European Research Council (P.P.D.F. and G. Scita), the Italian Ministries of Education, Universities, and Research (MIUR) and Health (P.P.D.F. and G. Scita), the Association for International Cancer Research (G. Scita and L.L.), the Ferrari Foundation (P.P.D.F.), the Monzino Foundation (P.P.D.F.), the CARIPLO Foundation (P.P.D.F. and G. Scita), and Fondazione Piemontese per la Ricerca sul Cancro-ONLUS-Intramural grant 5X1000 2008 (L.L.).

Received: July 20, 2012
Revised: September 2, 2013
Accepted: September 30, 2013
Published: November 14, 2013

### References

1. Zaidel-Bar, R., Itzkovitz, S., Ma'ayan, A., Iyengar, R., and Geiger, B. (2007). Functional atlas of the integrin adhesome. Nat. Cell Biol. *9*, 858–867.

2. Ridley, A.J., Schwartz, M.A., Burridge, K., Firtel, R.A., Ginsberg, M.H., Borisy, G., Parsons, J.T., and Horwitz, A.R. (2003). Cell migration: integrating signals from front to back. Science *302*, 1704–1709.
3. Valdembri, D., and Serini, G. (2012). Regulation of adhesion site dynamics by integrin traffic. Curr. Opin. Cell Biol. *24*, 582–591.
4. Pellinen, T., Arjonen, A., Vuoriluoto, K., Kallio, K., Fransen, J.A., and Ivaska, J. (2006). Small GTPase Rab21 regulates cell adhesion and controls endosomal traffic of beta1-integrins. J. Cell Biol. *173*, 767–780.
5. Ezratty, E.J., Bertaux, C., Marcantonio, E.E., and Gundersen, G.G. (2009). Clathrin mediates integrin endocytosis for focal adhesion disassembly in migrating cells. J. Cell Biol. *187*, 733–747.
6. Valdembri, D., Caswell, P.T., Anderson, K.I., Schwarz, J.P., König, I., Astanina, E., Caccavari, F., Norman, J.C., Humphries, M.J., Bussolino, F., and Serini, G. (2009). Neuropilin-1/GIPC1 signaling regulates alpha5beta1 integrin traffic and function in endothelial cells. PLoS Biol. *7*, e25.
7. Ezratty, E.J., Partridge, M.A., and Gundersen, G.G. (2005). Microtubule-induced focal adhesion disassembly is mediated by dynamin and focal adhesion kinase. Nat. Cell Biol. *7*, 581–590.
8. Chao, W.T., and Kunz, J. (2009). Focal adhesion disassembly requires clathrin-dependent endocytosis of integrins. FEBS Lett. *583*, 1337–1343.
9. Mai, A., Veltel, S., Pellinen, T., Padzik, A., Coffey, E., Marjomäki, V., and Ivaska, J. (2011). Competitive binding of Rab21 and p120RasGAP to integrins regulates receptor traffic and migration. J. Cell Biol. *194*, 291–306.
10. Zerial, M., and McBride, H. (2001). Rab proteins as membrane organizers. Nat. Rev. Mol. Cell Biol. *2*, 107–117.
11. Caswell, P.T., Vadrevu, S., and Norman, J.C. (2009). Integrins: masters and slaves of endocytic transport. Nat. Rev. Mol. Cell Biol. *10*, 843–853.
12. Yuan, L., Fairchild, M.J., Perkins, A.D., and Tanentzapf, G. (2010). Analysis of integrin turnover in fly myotendinous junctions. J. Cell Sci. *123*, 939–946.
13. Mendoza, P., Ortiz, R., Díaz, J., Quest, A.F., Leyton, L., Stupack, D., and Torres, V.A. (2013). Rab5 activation promotes focal adhesion disassembly, migration and invasiveness of tumor cells. J Cell Sci.
14. Sandri, C., Caccavari, F., Valdembri, D., Camillo, C., Veltel, S., Santambrogio, M., Lanzetti, L., Bussolino, F., Ivaska, J., and Serini, G. (2012). The R-Ras/RIN2/Rab5 complex controls endothelial cell adhesion and morphogenesis via active integrin endocytosis and Rac signaling. Cell Res. *22*, 1479–1501.
15. Jékely, G., Sung, H.H., Luque, C.M., and Rørth, P. (2005). Regulators of endocytosis maintain localized receptor tyrosine kinase signaling in guided migration. Dev. Cell *9*, 197–207.
16. Palamidessi, A., Frittoli, E., Garré, M., Faretta, M., Mione, M., Testa, I., Diaspro, A., Lanzetti, L., Scita, G., and Di Fiore, P.P. (2008). Endocytic trafficking of Rac is required for the spatial restriction of signaling in cell migration. Cell *134*, 135–147.
17. Stenmark, H. (2009). Rab GTPases as coordinators of vesicle traffic. Nat. Rev. Mol. Cell Biol. *10*, 513–525.
18. Frasa, M.A., Koessmeier, K.T., Ahmadian, M.R., and Braga, V.M. (2012). Illuminating the functional and structural repertoire of human TBC/RABGAPs. Nat. Rev. Mol. Cell Biol. *13*, 67–73.
19. Lanzetti, L., Rybin, V., Malabarba, M.G., Christoforidis, S., Scita, G., Zerial, M., and Di Fiore, P.P. (2000). The Eps8 protein coordinates EGF receptor signalling through Rac and trafficking through Rab5. Nature *408*, 374–377.
20. Lanzetti, L., Palamidessi, A., Areces, L., Scita, G., and Di Fiore, P.P. (2004). Rab5 is a signalling GTPase involved in actin remodelling by receptor tyrosine kinases. Nature *429*, 309–314.
21. Haas, A.K., Fuchs, E., Kopajtich, R., and Barr, F.A. (2005). A GTPase-activating protein controls Rab5 function in endocytic trafficking. Nat. Cell Biol. *7*, 887–893.
22. Haas, A.K., Yoshimura, S., Stephens, D.J., Preisinger, C., Fuchs, E., and Barr, F.A. (2007). Analysis of GTPase-activating proteins: Rab1 and Rab43 are key Rabs required to maintain a functional Golgi complex in human cells. J. Cell Sci. *120*, 2997–3010.
23. Rämet, M., Manfruelli, P., Pearson, A., Mathey-Prevot, B., and Ezekowitz, R.A. (2002). Functional genomic analysis of phagocytosis and identification of a *Drosophila* receptor for *E. coli*. Nature *416*, 644–648.
24. Scholpp, S., and Brand, M. (2004). Endocytosis controls spreading and effective signaling range of Fgf8 protein. Curr. Biol. *14*, 1834–1841.
25. Schiller, H.B., Friedel, C.C., Boulegue, C., and Fässler, R. (2011). Quantitative proteomics of the integrin adhesome show a myosin II-dependent recruitment of LIM domain proteins. EMBO Rep. *12*, 259–266.
26. Kuo, J.C., Han, X., Hsiao, C.T., Yates, J.R., 3rd, and Waterman, C.M. (2011). Analysis of the myosin-II-responsive focal adhesion proteome reveals a role for β-Pix in negative regulation of focal adhesion maturation. Nat. Cell Biol. *13*, 383–393.
27. Lanzetti, L., Margaria, V., Melander, F., Virgili, L., Lee, M.H., Bartek, J., and Jensen, S. (2007). Regulation of the Rab5 GTPase-activating protein RN-tre by the dual specificity phosphatase Cdc14A in human cells. J. Biol. Chem. *282*, 15258–15270.
28. Bazzoni, G., Shih, D.T., Buck, C.A., and Hemler, M.E. (1995). Monoclonal antibody 9EG7 defines a novel beta 1 integrin epitope induced by soluble ligand and manganese, but inhibited by calcium. J. Biol. Chem. *270*, 25570–25577.
29. Clark, K., Pankov, R., Travis, M.A., Askari, J.A., Mould, A.P., Craig, S.E., Newham, P., Yamada, K.M., and Humphries, M.J. (2005). A specific alpha5beta 1-integrin conformation promotes directional integrin translocation and fibronectin matrix formation. J. Cell Sci. *118*, 291–300.
30. Humphries, J.D., Byron, A., and Humphries, M.J. (2006). Integrin ligands at a glance. J. Cell Sci. *119*, 3901–3903.
31. Simonsen, A., Lippé, R., Christoforidis, S., Gaullier, J.M., Brech, A., Callaghan, J., Toh, B.H., Murphy, C., Zerial, M., and Stenmark, H. (1998). EEA1 links PI(3)K function to Rab5 regulation of endosome fusion. Nature *394*, 494–498.
32. Barbieri, M.A., Roberts, R.L., Gumusboga, A., Highfield, H., Alvarez-Dominguez, C., Wells, A., and Stahl, P.D. (2000). Epidermal growth factor and membrane trafficking. EGF receptor activation of endocytosis requires Rab5a. J. Cell Biol. *151*, 539–550.
33. Liu, J., Lamb, D., Chou, M.M., Liu, Y.J., and Li, G. (2007). Nerve growth factor-mediated neurite outgrowth via regulation of Rab5. Mol. Biol. Cell *18*, 1375–1384.
34. Bucci, C., Parton, R.G., Mather, I.H., Stunnenberg, H., Simons, K., Hoflack, B., and Zerial, M. (1992). The small GTPase rab5 functions as a regulatory factor in the early endocytic pathway. Cell *70*, 715–728.
35. Stenmark, H., Parton, R.G., Steele-Mortimer, O., Lütcke, A., Gruenberg, J., and Zerial, M. (1994). Inhibition of rab5 GTPase activity stimulates membrane fusion in endocytosis. EMBO J. *13*, 1287–1296.
36. Ginsberg, M.H., Partridge, A., and Shattil, S.J. (2005). Integrin regulation. Curr. Opin. Cell Biol. *17*, 509–516.
37. Roberts, M., Barry, S., Woods, A., van der Sluijs, P., and Norman, J. (2001). PDGF-regulated rab4-dependent recycling of alphavbeta3 integrin from early endosomes is necessary for cell adhesion and spreading. Curr. Biol. *11*, 1392–1402.
38. Zeigerer, A., Gilleron, J., Bogorad, R.L., Marsico, G., Nonaka, H., Seifert, S., Epstein-Barash, H., Kuchimanchi, S., Peng, C.G., Ruda, V.M., et al. (2012). Rab5 is necessary for the biogenesis of the endolysosomal system in vivo. Nature *485*, 465–470.
39. Teckchandani, A., Toida, N., Goodchild, J., Henderson, C., Watts, J., Wollscheid, B., and Cooper, J.A. (2009). Quantitative proteomics identifies a Dab2/integrin module regulating cell migration. J. Cell Biol. *186*, 99–111.
40. Foxman, E.F., Kunkel, E.J., and Butcher, E.C. (1999). Integrating conflicting chemotactic signals. The role of memory in leukocyte navigation. J. Cell Biol. *147*, 577–588.
41. Laukaitis, C.M., Webb, D.J., Donais, K., and Horwitz, A.F. (2001). Differential dynamics of alpha 5 integrin, paxillin, and alpha-actinin during formation and disassembly of adhesions in migrating cells. J. Cell Biol *153*, 1427–1440.
42. Laflamme, C., Assaker, G., Ramel, D., Dorn, J.F., She, D., Maddox, P.S., and Emery, G. (2012). Evi5 promotes collective cell migration through its Rab-GAP activity. J. Cell Biol. *198*, 57–67.
43. Assaker, G., Ramel, D., Wculek, S.K., González-Gaitán, M., and Emery, G. (2010). Spatial restriction of receptor tyrosine kinase activity through a polarized endocytic cycle controls border cell migration. Proc. Natl. Acad. Sci. USA *107*, 22558–22563.
44. Levéen, P., Pekny, M., Gebre-Medhin, S., Swolin, B., Larsson, E., and Betsholtz, C. (1994). Mice deficient for PDGF B show renal, cardiovascular, and hematological abnormalities. Genes Dev. *8*, 1875–1887.
45. Serio, G., Margaria, V., Jensen, S., Oldani, A., Bartek, J., Bussolino, F., and Lanzetti, L. (2011). Small GTPase Rab5 participates in chromosome congression and regulates localization of the centromere-associated protein CENP-F to kinetochores. Proc. Natl. Acad. Sci. USA *108*, 17337–17342.